FEB 1 ...

Aerosol Deposition and Losses in Two Alpha Air Monitors

A. H. Biermann and S. R. Sawyer

November 27, 1985

Lawrence Livermore National Laboratory

MASTER

AEROSOL DEPOSITION AND LOSSES IN
2 ALPHA-AIR MONITORS

A. H. Biermann and S. R. Sawyer

Hazards Control Department
Lawrence Livermore National Laboratory
Livermore, California 94550

Abstract

We assessed particle deposition and loss occurring in two alpha-air
monitors: an Eberline Alpha-3 Continuous Air Monitor (CAM) and a working-area
transuranic aerosol monitor (WOTAMS). We investigated the dependence of
particle size on losses in the sampling inlets and the real-time alpha
detector areas for both instruments. We determined the uniformity of particle
deposition on the filter to ascertain the effectiveness of the detector and
collection-filter configuration. Results indicate that particle losses are a
strong function of particle size in the CAM unit, with a 44% loss occurring
for 6-μm-diameter aerosols and a 0.3% loss for 0.6-μm-diameter aerosols.
Losses in the WOTAMS were less than 1% for particle diameters in the 0.6-to-7
μm range.

Introduction

We assessed the particle deposition and loss occurring in two alpha-air
monitors: an Eberline Alpha-3 Continuous Air Monitor (CAM), and a working area
transuranic aerosol monitor (WOTAMS). The CAM is commercially available, and
the WOTAMS is a prototype under development at Lawrence Livermore National
Laboratory (LLNL). In both instruments, we investigated the dependence of
particle size on losses in the sampling inlets and real-time alpha detector
areas. We determined the uniformity of particle deposition on the collection
filter to ascertain the effectiveness of the detector and filter physical
configuration. Also, since the lower limit of detection increases with
volumetric sample flow, we were interested in determining whether higher flows
were detrimental with respect to particle losses.

Experimental Procedure

Monodisperse aerosols of dioctylsebacate (DOS) and methylene blue (MB) were generated using a Berglund-Liu aerosol generator (Thermo Systems, Model-3050). This generator uses a vibrating orifice to produce uniformly sized droplets from a pressurized liquid solution. Filtered air is introduced for proper droplet dispersal and evaporation of the solvent, leaving the solute, either a solid or nonvolatile liquid, as the aerosol particle. The concentration of the solution and the size of the orifice determine the final aerosol particle size. Monodisperse aerosols can be produced that have geometric standard deviations of less than 1.1. We typically used three monodisperse aerosols with geometric, mean aerodynamic diameters ranging from 0.6 to 8 μm. Aerosols were monitored using either an optical particle counter (Climet-208) or a aerodynamic particle analyze (Thermo Systems, Model-3300). Aerosols below 2 μm in diameter were solid particles composed of MB. Aerosols larger than 2 μm in diameter were liquid DOS particles containing MB as a tracer for analysis.

The CAM contained a 47-mm diameter, cellulose membrane filter with a pore diameter of 5 μm. Two sampling flow rates of 11 and 40 lpm were tested for the three test aerosols. For the WOTAMS monitor, we used a 5.08-cm diameter, Millipore fluoropore filter with a pore size of 1.2 μm diameter. Flows of 50 and 113-142 liters/min were tested. In the WOTAMS experiments, both a large (34-mm diameter) and a small (17-mm diameter) detector were investigated. We also conducted experiments varying the detector-to-collection filter separation from 0.5 to 2 cm.

Aerosol particles deposited on the surfaces of the sampling systems in either the CAM or WOTAMS were removed by repeated swipes or washings with acetone or isopropyl alcohol. A spectrophotometer was used to measure the absorbance of MB to quantify particle deposition. Collection filters were sectioned into different areas to determine particle-concentration profiles across the filter surface.

Results and Discussion

We measured the amount of particle deposition for eight different portions
of the CAM chamber, including the collection filter. Figure 1 shows the
location of these collection areas. Table 1 lists the deposition that
occurred in these areas for the three monodisperse aerosols at the two flow
rates. Deposition values are given as percentages relative to the total mass
of MB retrieved from all CAM surfaces and the collection filter.

Collection on the filter varied from 99.7% of the particle deposits
retrieved for the smallest size aerosol (0.6 μm) at low flow, to 46% at the
largest particle size (6 μm) and low flow, to only 13% for the largest aerosol
size and high flow rate. In the large particle cases, most of the particles
not collected on the filter were collected in an area immediately above the
detector underneath the sample inlet port. The majority of these large
particles cannot follow the flow streamlines in this area and simply impact
onto this surface. Other losses include the chamber walls, especially for the
high flow case. No dominant areas of particle losses were seen for the
submicron aerosols.

Deposits on the collection filter were very non-uniform, especially for
the larger particle sizes. The main area of collection was in an area
opposite the inlet tube and the area of impaction above the detector as
previously described. Since the detector itself is only 25 mm in diameter, as
opposed to the 47-mm-diameter filter, it is important to ascertain the
detector efficiency for areas of the filter lying outside the projected area
of the detector onto the filter.

For this reason, a radioactive source was moved across the filter surface
to determine the spatial calibration of the detector with respect to distance
from the filter center. By integrating the product of this spatial calibra-
tion and the particles collection in different areas of the filter, we can
estimate what fraction of particles are actually detected. These numbers are
also presented in Table 1 in the row designated as "Estimated Amount
Detected." Even though great non-homogeneities in particle deposits were
observed on the filter surface, these are largely cancelled by the detector-
area integration. And even though we have seen greater particle losses at the
higher flow rate, the detector actually sees more particles at this higher

flow condition.

Turning to the WOTAMS, we analyzed particle deposits in the five areas shown in Figure 2. These included the inlet probe walls, a conical flowstream divider above the detector, the side walls of this flow divider, a simulated detector, the flow-divider support arms, and the detector face. Results for the largest aerosol case of 6-7 μm diameter are presented in Table 2 for various detector configurations and flow conditions. Again, depositions are expressed in percentages relative to the particle collection on all surfaces plus the sum of all collection filters used throughout the experiment. Total particle deposit is very minimal for all configurations. No losses were detected on the probe walls. Highest losses occurred for the detector support arms and flow divider. The smaller diameter detector at the lower flow condition had the smallest wall loss. Particle losses (not shown) for the smaller test aerosol were also minimal.

Deposits on the WOTAMS collection filters showed less concentrated areas immediately beneath the detector and areas of greater concentration outside the detector area. Minimum concentration depressions were about 20% below ideal uniform coverage for cases of the small detector configuration or large detector at 2-cm spacing. Concentrations falling to 80% below uniform coverage occurred for the larger detector at 0.5-cm spacings and at higher flow conditions. The effect of these non-uniform deposits on the WOTAMS detector performance have been previously discussed (Kaifer et al., 1985)

Conclusions

We observed significant particle losses in the CAM sampling systems for particles greater than 2 μm in diameter. These losses were more pronounced at higher sample rates but do not outweigh the benefits of the increased sample size. Non-uniform collection occurs on the filter, but this is largely inte- grated out by the radiation detector. Amounts actually seen by the detector vary from 4 to 35% depending on the aerosol size and sample flow rate.

In the case of the WOTAMS sampler, particle wall losses were minimal, or less than 0.5%, for aerosol diameters up to 8 μm. The higher flow rate of 140 liters/min seems acceptable; no significant increases in particle losses were

noticed. However, as in the case of the CAM, we did see concentration gradients across the filter due to the detector and support structure. It is probable that smaller and more rounded support arms could reduce these gradients.

References

R.C. Kaifer, J.F. Kordas, P.L. Phelps, C.T. Prevo, A.H. Biermann, D.W. Rueppel, D.L. Sawyer, R.M. Del Vasto, T.J. Merrill, and R.E. Salbeck (1985). "A Transuranic-Aerosol-Measurement System for the Workplace or Stack Monitoring," Presented at the I.E.E.E. Nuclear Science Symposium, San Francisco, CA, October 22-25, 1985.

Acknowledgments

Table 1. Aerosol deposition in the CAM for three monodisperse aerosols.

Aerodynamic Diameter (m)	Low Flow			High Flow		
	5.95	2.65	0.64	5.80	2.08	0.74
Location	% of total deposits					
Inlet tube	0.6	0.4	0.06	1.7	2.0	0.6
Inlet tube, bottom	2.1	1.8	0.07	2.9	4.5	1.1
Area above detector	44.0	0.5	0.06	74.5	21.8	1.4
Area around detector	1.9	0.1	0.04	0.4	2.4	0.4
Rest of chamber	4.7	0.6	0.05	7.3	8.1	0.6
Filter retainer ring	0.5	0.5	0.03	0.4	0.7	0.4
Detector face	0.05	0.1	0.03	0.0	0.4	0.4
Filter	46.2	96.0	99.7	12.8	60.7	95.5
Estimated Amount Detected	15	32	35	4	21	45

Table 2. Particle Deposition in the WOTAMS for 6-8 μm aerosols.

Detector Spacing (cm) Flow Rate (1pm)	Large 0.5 113	Small 0.5 141	Large 2 141	Small 2 141	Large 0.5 57
Location					
Probe wall	0.0	0.0	0.0	0.0	0.0
Detector support	0.07	0.25	0.10	0.0	0.0
Flow divider, front	0.11	0.0	0.1	0.06	0.01
Flow Divider, sides	0.07	0.01	0.14	0.04	0.04
Detector face	0.03	0.0	0.0	0.0	0.0
Total deposition	0.28	0.26	0.34	0.10	0.05

Figure Captions

Figure 1.   CAM chamber showing the collection areas.

Figure 2.   A cross-sectional view of the WOTAMS inlet probe, illustrating the
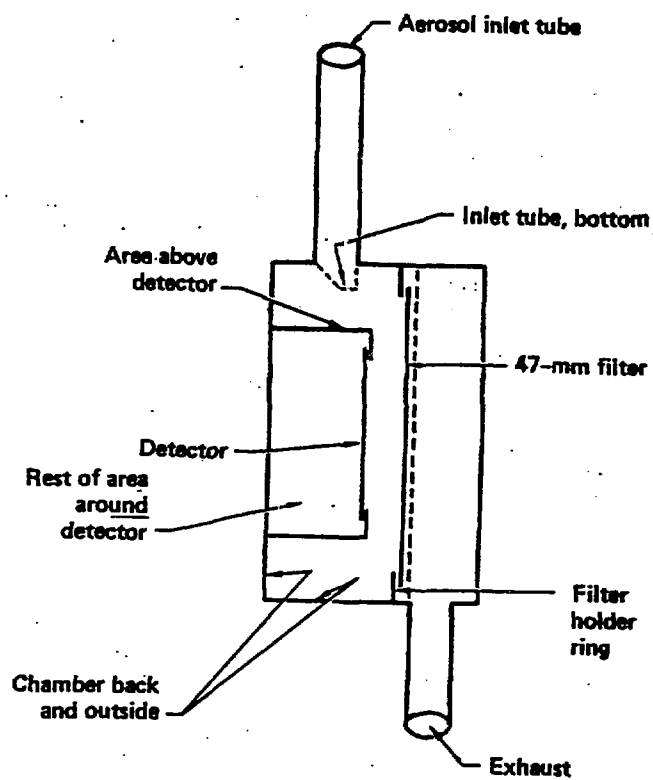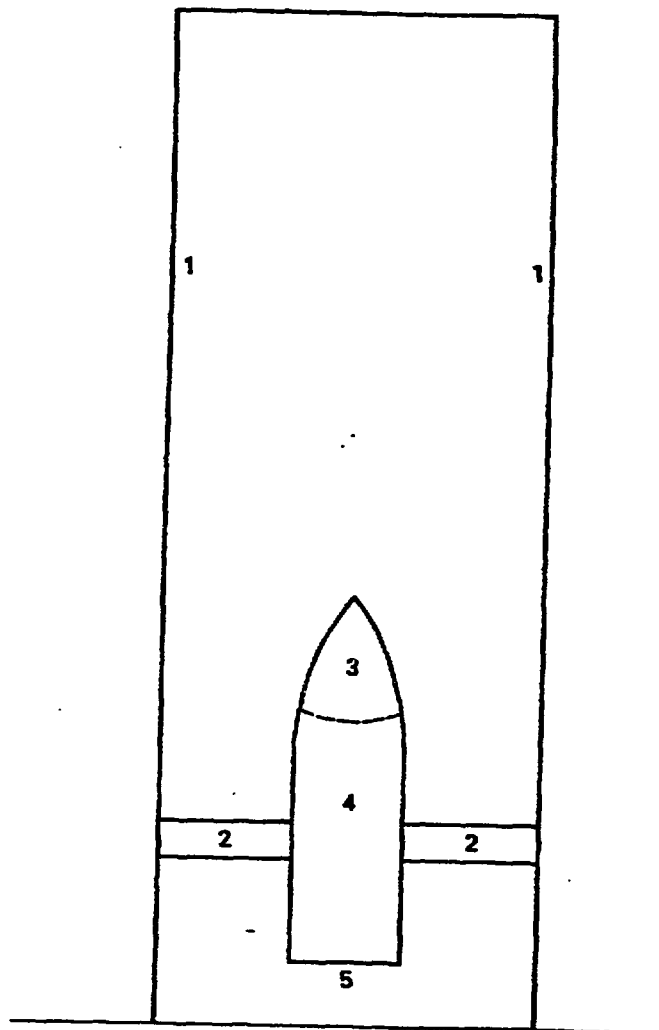   areas analyzed for particle deposition.

Figure 1.   CAM chamber and collection areas.

1. Probe wall
2. Detector support
3. Detector flow divider, cone portion
4. Detector flow divider, sides
5. Detector face

Fig. 2.   A cross-section view of the WOTAMS inlet probe illustrating
the areas analyzed for particle deposition.